Ligands make the difference! Molecular insights into CrVI/SiO2 Phillips catalyst during ethylene polymerization

UNIVERSITÀ DEGLI STUDI DI TORINO

Ligands make the difference! Molecular insights into Cr^{VI}/SiO_2 Phillips catalyst during ethylene polymerization.

Caterina Barzan,[a]* Alessandro Piovano,[a] Luca Braglia,[a,b] Giorgia A. Martino,[a] Carlo Lamberti,[a,b] Silvia Bordiga[a] and Elena Groppo[a]*

[a] Department of Chemistry, University of Turin, Via G. Quarello 15A, I10135, Italy

[b] IRC "Smart Materials", Southern Federal University, Zorge Street 5, 344090 Rostov-on-Don, Russia

KEYWORDS: Phillips catalyst, Ethylene polymerization, Chromium, Methylformate, Operando spectroscopy.

ABSTRACT: *Operando* sensitive spectroscopic techniques were employed for investigating the changes in the molecular structure of the Cr sites in the Cr^{VI}/SiO_2 Phillips catalyst during ethylene polymerization. Practically, the most arduous barrier to be overcome was the separation of the chromates reduction carried by ethylene from the subsequent polymerization. By carefully tuning the experimental parameters, we succeeded in observing these two events separately. We found that the sites active in ethylene polymerization are mainly divalent Cr ions in a 6-fold coordination, in interaction with the oxygenated by-product (methylformate, generated from the disproportionation of two formaldehyde molecules). Un-reduced Cr^{VI} species are also present during ethylene polymerization as well as reduced Cr species (either Cr^{II} or Cr^{III}) acting as spectators. Our results challenge the old vision of "naked" chromium species (i.e. low coordinated) as the active sites, and attribute a fundamental role to external (and flexible) oxygenated ligands, that resemble the ancillary ligands in homogeneous polymerization catalysis.

1. INTRODUCTION

Back in 1951, Hogan and Banks at the Phillips Petroleum discovered a Cr-based catalyst for ethylene polymerization and named it after their Company.[1] Since then, the Phillips catalyst has been successfully used in the commercial production of high-density and linear low density polyethylene (HDPE and LLDPE). Today the predictions of the global demand for polyethylene resins settles at 4.0 percent rise per year to 99.6 million tons in 2018, valued at $164 billion.[2] In this market the Phillips catalyst supplies almost 40% of the HDPE total world demand, thanks to its versatility in terms of hundreds of specialized PE grades produced, resulting in just as many specific applications ranging from packaging to medical and automotive sectors.[3-5] The catalyst synthesis consists in the impregnation of a polymer-grade porous silica with a Cr precursor (loadings lower than 1 wt%), followed by calcination at high temperature (> 500 °C).[3,6-10] This procedure gives a highly dehydroxylated silica where the chromium ions are grafted mainly as isolated hexavalent chromates[6,9-20] (hereafter Cr^{VI}), although also mono-oxo CrO_5 species have been claimed in the recent literature.[21-29] These chromium species are just the precursors of the active sites. Indeed, once ethylene is introduced in the reactor at temperatures from 80 to 110 °C, it reduces the Cr^{VI} sites during a variable induction period, forming reduced Cr species active in ethylene polymerization and some oxidation by-products. Formaldehyde has been long claimed as the main ethylene oxidation by-product and experimentally detected in a few cases.[7,8,30-33] In contrast, the nature of the reduced Cr sites (in terms of molecular structure, oxidation state, local geometry) has been the subject of a long debate in the past[3,6-10,34] and has recently gained a renewed attention in the high level specialized literature, fostering a great number of experimental[22,23,35-40] and theoretical[24-29,41-44] studies. Most of the recent works are focused on the long-standing question of the chromium oxidation state. In fact, while Cr^{II} sites were invoked as the active sites since the early literature on the Phillips catalyst[45-49] and successively proved by many experimental studies,[3,6-9] Cr^{III} is coming back to researchers attention after a series of papers by Coperet et al.,[35,36,43,44,50,51] who showed that Phillips-inspired Cr^{III}/SiO_2 catalysts obtained from well-defined Cr^{III} precursors are active in ethylene polymerization. These new results opened the way to the modeling of a large number of reaction pathways aimed at explaining the spontaneous self-alkylation mechanism in the presence of ethylene,[41,42,44,50] that has long remained unknown.

In this animated debate on the chromium oxidation state and polymerization mechanism distracts the attention from the molecular structure of the active chromium sites. Traditionally, they have been considered as relatively "naked", irrespective of their oxidation state, and highly uncoordinated Cr sites have been indeed used to model the polymerization mechanism.[41-44] It is worth addressing the word "naked" as a vision of extremely low coordinated Cr sites, which are mostly represented covalently bonded to two or three O-Si from the silica surface. At most, surrounding hemilabile siloxane groups have been considered to enter into the Cr coordination sphere.[41,52] While the vision of "naked" Cr sites might be plausible for the pre-reduced Phillips catalysts or for Cr-based catalysts derived from well-defined organometallic precursors, it appears less straightforward for Cr^{VI}/SiO_2 reduced in ethylene, where the active sites are formed at ca. 100 °C in the presence of ethylene and of the oxidation by-

products. The present work has the intention to provide new insights into the molecular structure of Cr^{VI}/SiO_2 during ethylene polymerization. Achieving this goal not only would represent a scientific milestone but also would be the key for the development of new concepts, and for the rational design of a new generation of olefin polymerization catalysts.[53]

Up to now, the main experimental difficulty was associated with the double role of ethylene as reducing agent and monomer. Several strategies were attempted to separate the formation of the active sites from the ethylene polymerization, as e.g. using an external reducing agent prior to ethylene injection,[3,9,10,38-40,54,55] or synthesizing Cr/SiO_2 catalysts starting from well-defined Cr^{VI-n} organometallic precursors.[35,36,51,56,57] Although these approaches gave a relevant contribution to the overall understanding of the Phillips catalyst, in most of the cases the obtained polyethylene is different with respect to that produced with the hexavalent Cr^{VI}/SiO_2 catalyst.[3] This implies that the molecular structure of the active Cr sites strongly depends on the pre-reducing process or synthesis methodology and that the only way to observe the real active sites in ethylene-reduced Cr/SiO_2 is to look carefully at it under the actual reaction conditions. *Operando* spectroscopic techniques have this potential and nowadays have progressed enough to be applied with success also on very dilute systems.[58-63]

On these bases, we propose here a detailed investigation on the formation and structure of the active sites in Cr^{VI}/SiO_2 based on the synergic use of three *operando* spectroscopic techniques – namely Cr K-edge XANES, Diffuse Reflectance (DR) UV-Vis-NIR and FT-IR spectroscopies (coupled with on-line MS) – assisted by state-of-the-art theoretical calculation. Although the three techniques have been already used in the investigation of the Phillips catalyst by several research groups (including some of us), the novelties of the present work rely on: 1) a careful tuning of the experimental parameters that allowed us distinguishing between the formation of the active sites and the starting of the polymerization, and 2) the multi-technique approach that allows monitoring at the same time the changes occurring at the Cr sites, the nature and location of the by-products, and the occurrence of ethylene polymerization.

2. RESULTS AND DISCUSSION

A synthetic panning shot of the most relevant spectroscopic results is shown in Figure 1, which displays the spectra collected during Cr^{VI}/SiO_2 reduction in the presence of ethylene (from black to red) and subsequent polymerization (from red to orange) at 150 °C.[64] Both XANES (Figure 1a) and DR UV-Vis-NIR (Figure 1c) indicate that the chromates[6,9,10,65,66] are gradually reduced. In the XANES spectra: i) the intense pre-edge peak centered at 5993.5 eV typical of pseudo-tetrahedral chromates[6,9,10,18,67-72] decreases in intensity and is gradually replaced by two very weak bands at 5989.8 and 5992.5 eV; ii) the edge progressively downward shifts from 6006.7 eV to 6002.0 eV, and iii) the white-line increases in intensity (pronounced peak at about 6011 eV) and the maximum at 6032 eV is replaced by a profound minimum. At the end of the experiment, the occurrence of ethylene polymerization was indicated by the appearance of the powder in the capillary: white and with a rubber consistence.[73] In the DR UV-Vis-NIR spectra the intense band at 21500 cm^{-1} (assigned to an O→Cr charge transfer transition localized mainly on the double bonded oxygen of the chromates)[6,9,10,15-20,65,66] gradually decreases in favor of two weaker bands at 9500 and 16700 cm^{-1} (with a shoulder at 15000 cm^{-1}) indicative of d-d transitions for Cr^{VI-n} species (Figure 1c').[6,9,10,24-29] After an induction time, the occurrence of ethylene polymerization on the reduced Cr sites is indicated by the appearance of a few narrow and weak bands in the 4400-4050 cm^{-1} region (Figure 1d"), due to the combination of the $\nu(CH_2)$ and $\delta(CH_2)$ vibrational modes of polyethylene.[35,43,74-80] The XANES and DR UV-Vis-NIR spectra after ethylene reduction contain important indications on the local geometry and oxidation state of the reduced Cr sites. The weakness of the two bands at 5989.8 and 5992.5 eV in the pre-edge region of the XANES spectrum as well as the weak intensity of the d-d bands in the UV-Vis spectrum point towards reduced Cr species characterized by a pseudo-octahedral coordination.[9,10,58,68,71,72]

A quick comparison of the XANES spectrum with that of a Cr^{III} reference compound might lead to the conclusion that the final oxidation state of the catalyst reduced in ethylene is +3. Indeed, at a first glance, the pre-edge features and edge position of Cr^{VI}/SiO_2 reduced in ethylene are very similar to those of Cr_2O_3 (Figure 2a), in which the Cr sites have an oxidation state of +3 and a 6-fold geometry. These (and similar) arguments have been used several times in the literature to set forth +3 as the main oxidation state of the Cr active sites.[35,36,43,51] However, Figure 2a demonstrates that the spectrum of Cr^{VI}/SiO_2 reduced in ethylene is also very similar to that of Cr^{VI}/SiO_2 reduced in cyclohexene at room temperature, where the Cr sites have an oxidation state of +2 in a 6-fold coordination environment due to the interaction with an ester (deriving from the oxidation of cyclohexene).[55] Notably, in that case EPR spectroscopy, which is selective towards Cr^{III}, incontrovertibly discarded the presence of Cr^{III}.[55] It clearly emerges that the assignment of the Cr oxidation state on the basis of *only* Cr K-edge XANES spectroscopy is not unambiguous. The same conclusion was reached several years ago by Tromp at al.,[72] who demonstrated that the position of the main absorption edge for a series of well-defined Cr^{III} complexes with different ligands and geometries can move as much as 8 eV (i.e. a shift comparable to that caused by a change in the oxidation state from +6 to 0).

Concerning the DR-UV-Vis –NIR spectra the bands at 9500 and 16700 cm^{-1} could be assigned either to Cr^{II} or to Cr^{III}, or both. From a survey of the specialized literature, the salts of trivalent 6-fold coordinated Cr ions give two bands around 17000 and 24000 cm^{-1} (and a third one , rather weak, at 37000 cm^{-1}, which is however always masked by the intense charge transfer band at high energy).[81] Cr^{II}

ions in a perfect octahedral environment give a broad and weak band between ca. 10000 and 20000 cm^{-1} (e.g. $Cr^{2+}(H_2O)_6$ shows a single $^5E_g \rightarrow {}^5T_{2g}$ transition around ca. 14000 cm^{-1}).[82] Upon distortion of the octahedral symmetry, this transition splits into multiple components. For Cr ions in a (largely) O-donor coordination sphere, d-d bands at wavenumbers as low as 9500 cm^{-1} are commonly assigned to Cr^{II} species. The presence of a band near 10000 cm^{-1} in the UV-Vis spectra of 6-fold-coordinated Cr^{II} complexes, especially discernable in DR mode, was noticed already in the 1960s.[81-83] According to these seminal works, the DR spectra of several octahedral distorted Cr^{II} salts show bands around 10000, 13100, 16000 and 18900 cm^{-1}. On these basis, our DR UV-Vis-NIR measurements clearly indicate that a large fraction of the reduced Cr sites are in the divalent state and in a 6-fold coordination, although the co-presence of also Cr^{III} species cannot be discarded. Further proof is given by a comparison of the DR UV-Vis-NIR spectra shown in Figure 2b (and completely discussed in Section S1) of the Cr^{VI}/SiO_2 catalyst reduced in ethylene before the polymerization starts (red) with that of the same catalyst reduced in cyclohexene at room temperature (light blue) and a reference for Cr^{III}/SiO_2 (green).

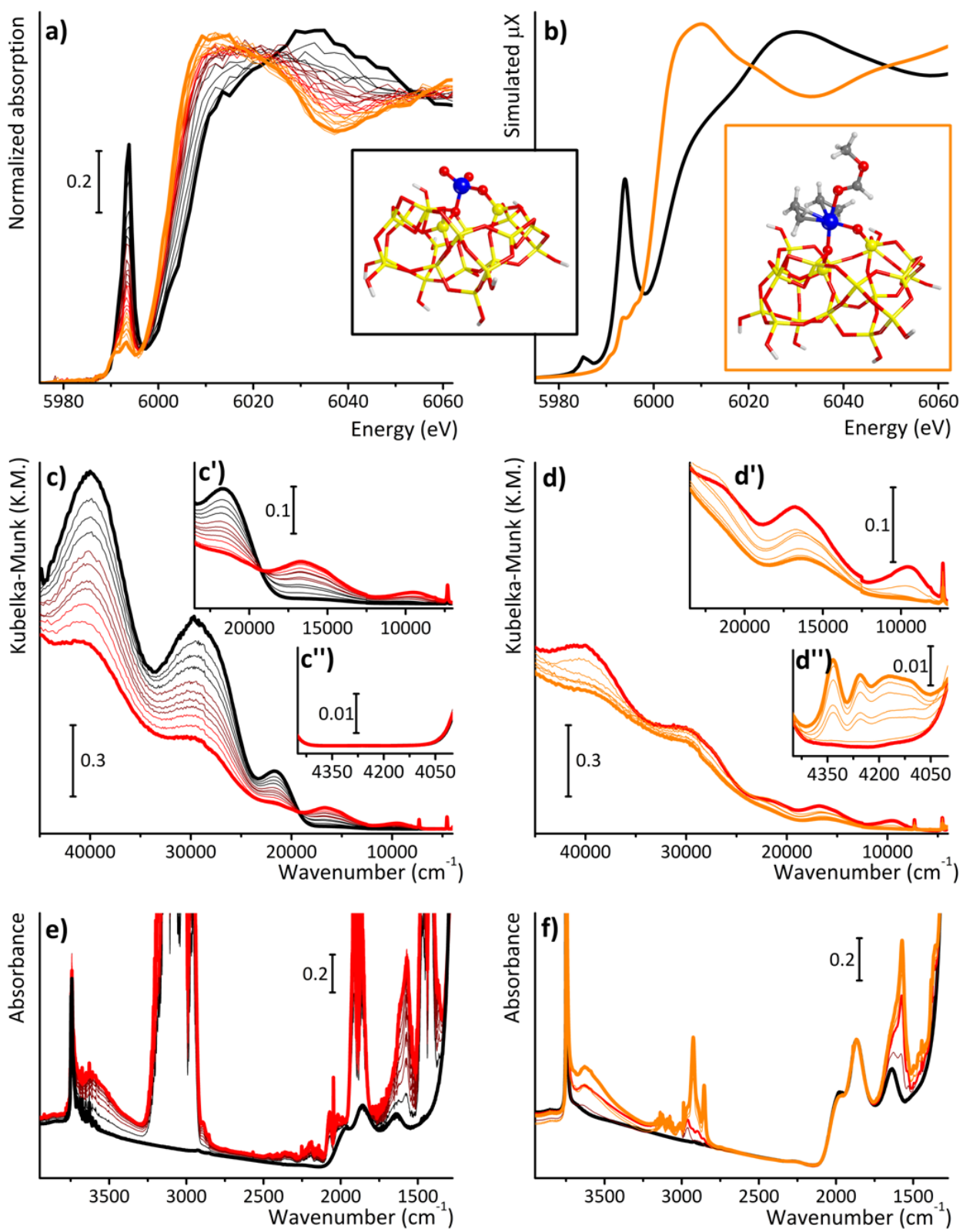

Figure 1. Time evolution of the spectra for the Cr^{VI}/SiO_2 catalyst (bold black) during reduction with ethylene (from black to bold red) and during ethylene polymerization at 150 °C (from red to bold orange). Part **(a):** Normalized Cr K-edge XANES spectra. Part **(b)**: Simulated XANES spectra of Cr^{VI}/SiO_2 (black) Cr^{II}/SiO_2 in interaction with methylformiate and ethylene (orange), and corresponding structural models. Part **(c)** and **(d)**: DR-UV-Vis-NIR spectra subdivided into the two reaction steps. Insets c'/d' and c"/d" show a magnification of the 24000-7000 cm^{-1} and 4400-4050 cm^{-1} regions, in which the d-d absorption bands and the $\nu(CH_2)$ and $\delta(CH_2)$ combination modes of PE are present, respectively. Part **(e)**: *Operando* FT-IR spectra. Part **(f)**: FT-IR spectra collected in static conditions.

Also in this case the d-d bands of the ethylene reduced Cr sites have positions and intensity ratios extremely similar with those obtained upon cyclohexene reduction, characterized by Cr^{II} 6-fold coordinated species in interaction with an ester molecule.[55] We wish to underline here that this assignment has been possible because the DR-UV-Vis spectra have been collected in a wide energy region comprising also the NIR range, which is neglected in most of the recent literature.[84]

Hence, our working hypothesis to account for these results is that *we are mainly detecting intermediate Cr^{II} species in a 6-fold coordination because in interaction with formaldehyde molecules,* which are the main ethylene oxidation by-products claimed in the literature.[7,8,30-33] However, to our surprise, only traces of masses diverse from ethylene were detected by online MS during both *operando* XANES and DR UV-Vis-NIR measurements, also for long reaction times.

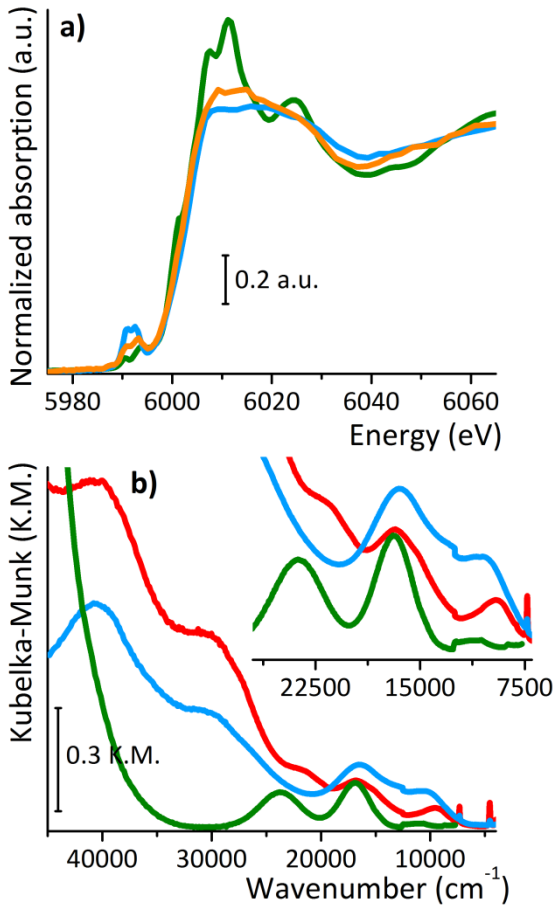

Figure 2. Part a) XANES spectrum of the Cr^{VI}/SiO_2 catalyst upon reduction and polymerization in ethylene (orange) in comparison with the spectrum of the same catalyst reduced in cyclohexene at room temperature (light blue)[55] and with the spectrum of the reference Cr_2O_3 oxide (green). Part b) DR UV-Vis-NIR spectrum of the Cr^{VI}/SiO_2 catalyst upon reduction and before ethylene polymerization occurs (red), compared with the same catalyst reduced at room temperature in cyclohexene (light blue)[55] and of the a Cr^{III} reference ($CrCl_3$*6(H_2O) complex physisorbed on Aerosil SiO_2, green spectrum).

The lack of observation of formaldehyde or of any other volatile oxidation by-product stimulated us to follow the same experiment by *operando* FT-IR spectroscopy, aimed at directly detecting possible oxygenated species released during the reduction of chromates and adsorbed at the catalyst surface. In the presence of ethylene at 150 °C (Figure 1e) a few IR absorption bands gradually grow at 2892 and 2865 cm^{-1} (typical IR region of $\nu(CH_x)$ modes), along with two more intense bands at 1617 and 1573 cm^{-1}. The assignment of these latter bands to vibrations involving oxygenated species is straightforward due to their extremely high intensity with respect to the $\nu(CH_x)$ modes. Indeed, only chemical groups with high extinction coefficient (such as organic carbonyls, formates and others) can result in such intense manifestations.[85-89] In principle, also the ν(C=C) mode can be invoked, however, this group has a low extinction coefficient with respect to the $\nu(CH_x)$ modes, and thus cannot be the guilty party.[74,77,90,91] A complete assignment of the IR absorption bands due to the adsorbed species can be done only by looking at the Mid-IR spectral region in its totality. This is not feasible during the *operando* FT-IR measurements, since the spectra are dominated by the absorption bands of gaseous ethylene and do not allow the observation of other spectroscopic fingerprints necessary for a complete assignment. To overcome this spectroscopic obstacle we performed a parallel FT-IR experiment in static conditions (150 °C, $P_{C_2H_4}$ = 100 mbar, Fig. 1f). By removing the gaseous contribution of ethylene, the chromate reduction becomes visible and is testified by the gradual decrease in intensity of the weak band at 1980 cm^{-1} due to the first overtone of the ν(Cr=O) vibrational mode[9,10,69,70,78,92] as clearly visible in Figure 3c. At the same time, new absorption bands grow before ethylene polymerization starts at 2955, 2892, 2865, 2747, 1617, 1573, 1455, 1383 and 1369 cm^{-1}. The complete assignment of each IR absorption band is shown in Table 1, along with the strength of the vibrational modes. These bands are assigned not to formaldehyde, but rather to vibrations of oxygenated molecules derived from a disproportionation of formaldehyde on the Cr^{II} sites. In particular, our most accredited species is methylformate, which is formed through the Tischenko reaction[55,85,93-97] of two formaldehyde molecules at the same Cr^{II} site. This assignment was provided both by referring to literature assignments in which methylformate is strongly bond to Lewis acid sites (ν(C=O) frequency can red shifts from 1720 cm^{-1} to even 100 cm^{-1} less)[85,98] but also by selectively dosing pure formaldehyde on SiO_2 and on a Cr^{II}/SiO_2 catalyst activated following the same route as the Cr^{VI}/SiO_2 catalyst. Details of surface reactions and assignment of the multiple products are largely discussed in Section S3. On the other hand, we cannot exclude alternative reaction paths leading to the formation of adsorbed formate species and methoxy groups grafted at the silica surface, that would lead to similar spectroscopic signa-

tures. This latter hypothesis is valid if the Cr sites remain bis-grafted to the silica surface.

Notably, these formate and methoxy species (methyl formate) are strongly interacting/bonded to the catalyst surface, since their IR absorption bands neither decrease in intensity in the operando/dynamic conditions (i.e. being removed by the ethylene flow or outgassing at 150 °C in UHV), nor shift at higher frequencies during the process (i.e. removed from the Cr site to the silica surface).

It is important to add to the discussion that attempts to extract the oxidized by-products by means of several solvents failed for Cr^{VI}/SiO_2 reduced by cyclohexene,[55] owing to the extremely high reactivity of the reduced catalyst towards the solvents themselves (or pollutants). In the present case, the scenario is even worse due to the difficulty in stopping the reaction before the occurrence of ethylene polymerization, and hence to the possible co-presence of polyethylene.

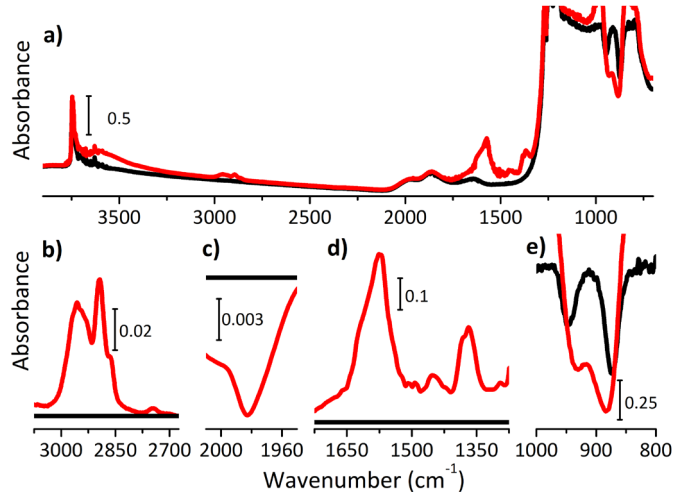

Figure 3. FT-IR spectra of Cr^{VI}/SiO_2 before (black) and after reduction in ethylene at 150 °C (red). Part (a) shows the spectra in the whole 3800–700 cm-1 wavenumber region; parts (b) and (d) show magnifications in the spectral regions where the absorption bands characteristic of ethylene oxidation products give a contribution (spectra subtracted from that of Cr^{VI}/SiO_2); part (c) shows the magnification of the region in which the first overtone of the Cr=O mode of the chromate species contributes (subtracted spectra); part (e) reports a magnification of the region where the vibrational modes of silica perturbed by the presence of the chromates are visible.

Table 1. Position (in wavenumbers, cm^{-1}) and relative intensity (vs = very strong, s = strong, m = medium, w = weak) of the IR absorption bands attributed to ethylene oxidation products in interaction with the ethylene reduced Cr^{VI}/SiO_2 catalyst

Observed bands (cm^{-1})	*Assignment*
2955 (s)	$\nu_{asymm}(OCO) + \delta(CH)$ / $\nu_{asymm}(CH_3)$
2892 (s)	$\nu_{symm}(CH_3)$
2865 (s)	$\nu(CH)$
2747 (w)	$\nu_{symm}(OCO) + \delta(CH)$
1617, 1573 (vs)	$\nu_{asymm}(OCO)$
1455 (m)	$\delta(CH_3)$
1383 (s)	$\delta(CH)$
1369 (vs)	$\nu_{symm}(OCO)$

Having identified the main oxidation state of the reduced Cr sites (by DR UV-Vis-NIR) and the main oxidation by-product (by FT-IR), we went back to the XANES spectra with the aim of getting rid of the interpretation ambiguity. We simulated the XANES spectra of several DFT-optimized Cr structures relevant for the discussion, by using the FDMNES code[99-101] (that uses the finite difference method to solve the Schrödinger equation) and self-consistent calculations (i.e without imposing any restriction on the shape of the potential such as the *muffin-tin* approximation).[102-104] The experimental XANES spectra of Cr^{VI}/SiO_2, Cr^{II}/SiO_2 and Cr_2O_3 (Section S2) are well reproduced by our structural models,[105] demonstrating the reliability of our method. The XANES spectrum of Cr^{VI}/SiO_2 at the end of the reaction (orange in Figure 1a) was simulated by a model of Cr^{II}/SiO_2 in interaction with methylformate and two molecules of ethylene (orange in Figure 1b). The main experimental features are very well reproduced by the model, further supporting our previous conclusions.[106]

Summarizing, the first relevant result emerging from our spectroscopic study is the *identification, during the reduction of Cr^{VI}/SiO_2 in ethylene, of 6-fold coordinated Cr^{II} species in interaction with a methylformate molecule*. This novel concept is in very well agreement with recent findings by McDaniel and co-workers, who demonstrated that under commercial ethylene polymerization conditions oxygenates may remain attached to the chromium sites.[107] The next questions are whether *these hindered Cr^{II} sites are active in ethylene polymerization and whether methylformate remains attached to the Cr sites during ethylene polymerization, participating to the whole reaction.* DR UV-Vis-NIR and FT-IR spectroscopies help in answering these questions.

In the DR UV-Vis-NIR spectra (Figure 1d, from red to orange) the start of ethylene polymerization (appearance of absorption bands in the 4400-4050 cm^{-1} range) is accompanied by a visible change in the scattering properties of the catalyst powder and by the decrease in intensity of the two d-d bands at 9500 and 16700 cm^{-1}. This concomitance clearly and strongly indicates *that the Cr^{II} species in interaction with the oxidized by-products are the active species involved in ethylene polymerization*. Interestingly, the decrease in intensity of the two d-d bands upon ethylene polymerization is not complemented by the growth of other bands. The reason is that polyethylene forms a white coating around the Cr/SiO_2 particles, which diffuses the incident light and shields the Cr active sites from the DR UV-Vis measurements. The effect is macroscopically visible in Figure 4, which shows the appearance of the activated Cr^{VI}/SiO_2 catalyst before, during reduction and after ethylene polymerization (from left to right, respec-

tively). The final spectrum (bold orange in Figure 1d) is characterized by a general low intensity due to the presence of polyethylene at the catalyst surface. Two bands at 21500 and 16000 cm^{-1} are still detectable. The band at 21500 cm^{-1} indicates the persistence of a few unreacted chromates, meaning that *ethylene polymerization proceeds in the presence of residual – slowly reducible – chromates*, in agreement with previous reports.[108,109] The band at 16000 cm^{-1} could be assigned to a d-d transition of another reduced Cr species not involved in polyethylene formation. Its position is compatible with both 6-fold coordinated Cr^{II} and Cr^{III} species.

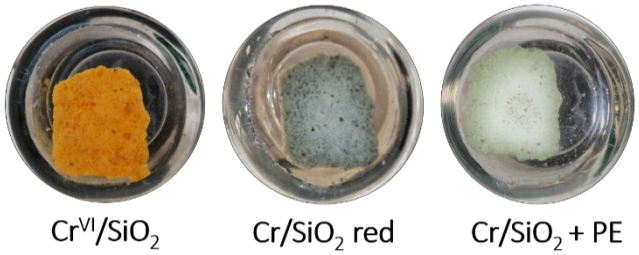

Figure 4. Pictures of the Cr^{VI}/SiO_2 catalyst pellet placed inside a quartz cell before, during reduction in ethylene and after polymerization (from left to right). The gradual increase of the light diffusion of the pellet is macroscopic and proves the loss of KM units in the whole DR UV-Vis-NIR spectra upon ethylene polymerization.

FT-IR spectroscopy (Fig. 1f) reveals that ethylene polymerization (characteristic polyethylene bands: $\nu_{asymm}(CH_2)$ at 2924, $\nu_{symm}(CH_2)$ at 2853 cm^{-1} and $\delta(CH_2)$ at 1472-1463 cm^{-1}) is consequent to the formation of methylformate. In addition, the absorption bands characteristic of methylformate are not affected by the polyethylene growth, testifying that *the oxidized by-products remain on the active Cr site also during the ethylene polymerization and have to be considered important participants in the catalysis*. As a side note, the IR absorption bands of methylformate keep on growing also during ethylene polymerization, confirming that the reaction starts in the presence of a residual fraction of Cr^{VI}.

As a final step, in Figure 5 we made an attempt to correlate the time evolution of all the species detected with all the techniques, which are involved in the reaction, namely: i) the starting Cr^{VI}, ii) the intermediate Cr^{II} in interaction with the oxygenated by-product iii) a reduced Cr species acting as spectator, iv) the polyethylene product and iv) the oxygenated by-product (methylformate). The spectroscopic fingerprints of Cr^{VI} were used to rescale the time vector for the three techniques. In the DR UV-Vis-NIR and FT-IR spectra the absorption bands characteristic of each species were easily deconvoluted and their intensity plotted as a function of time. In contrast, for XANES a principal component analysis (PCA) followed by a Multivariate Curve Resolution - Alterning Least Squares (MCR-ALS) was applied to the whole sequence of spectra (Section S4). The analysis resulted in three principal components, corresponding to Cr^{VI}, Cr^{II} in interaction with the oxygenated by-product and a reduced Cr species behaving as a spectator. The border between the reduction and the polymerization steps was traced on the basis of the UV-Vis and FT-IR results.

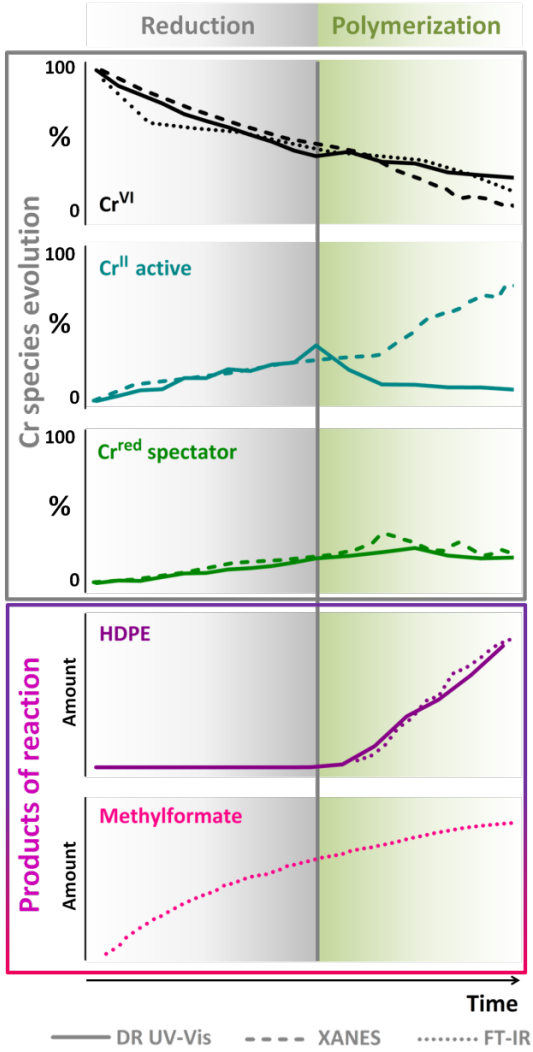

Figure 5. Time evolution of the DR UV-Vis-NIR (solid lines), XANES (dashed lines) and FT-IR (dotted lines) spectroscopic fingerprints of: i) **Cr^{VI}** (21500 cm^{-1} UV-Vis – 1980 cm^{-1} FT-IR – first component in PCA XANES); ii) **Cr^{II}** in interaction with methylformate and ethylene (9500 cm^{-1} UV-Vis – second component in PCA XANES); iii) **spectator Cr** (15100 cm^{-1} UV-Vis – third component in PCA XANES); iv) **HDPE** (4400-4050 cm^{-1} UV-Vis – 2853 cm^{-1} FT-IR); v) **methylformate** (1573 cm^{-1} FT-IR).

The data summarized in Figure 5 allow stating the following additional conclusions:

a) During the reduction step, Cr^{VI} are converted into Cr^{II} sites in interaction with the oxygenated by-product (methylformate), and into a reduced Cr species that does not participate to the reaction.
b) Ethylene polymerization starts on the Cr^{II} sites, but in the presence of residual Cr^{VI} sites, which are slowly reduced in the successive time.

c) The Cr^{II} sites active in ethylene polymerization are rapidly buried in the produced polymer and become invisible for DR UV-Vis-NIR spectroscopy, but are still visible with XAS. These sites are continuously formed even during the polymerization, to the expenses of the residual Cr^{VI} and with the concomitant formation of methylformate.

3. CONCLUSIONS

Extremely focused spectroscopic investigations of the Cr^{VI}/SiO_2 Phillips catalyst in *operando* conditions have been the key to unravel the molecular structure of the Cr sites active in ethylene polymerization. Our new spectroscopic evidences reveal that the *chromium site active in ethylene polymerization is a divalent ion, 6-fold coordinated and in interaction with an external nucleophilic ligand (methylformate)*. This study provides the first spectroscopic identification, at the molecular level, of the oxygenated species adsorbed on the catalyst during the induction period inferred by indirect TG, DSC and MS experiments.[107] We also introduce the important concept that oxygenates remain in the Cr coordination sphere also *during* ethylene polymerization. Additionally, we demonstrate that ethylene polymerization occurs also if a fraction of the chromate sites is not reduced, implying that Cr^{VI} sites might have a role in the first steps of the catalysis in cooperation with the active Cr^{II} sites, as already proposed in the literature.[108,109] This cooperation might be due to higher strain effects[110] caused by the chromate sites (i.e. $[SiO]_2CrO_2$ sites have shorter Cr-O bonds with respect to their reduced counterparts)[52] on the already formed Cr reduced species.

We wish to underline that each technique employed in this work, if taken as a single measurement, cannot lead to safe statements on the molecular structure of the Cr sites. On the other hand, the totality of the results collected with each spectroscopic technique converge to a single picture in which the Cr^{II} sites 6-fold coordinated are those involved in the reaction, while a fraction of reduced Cr sites acts as spectator. This is valid for Cr^{VI}/SiO_2 directly reduced in ethylene. We reiterate that in our opinion both "naked" Cr^{II} and Cr^{III} sites may be active in ethylene polymerization, as for ad-hoc reduced catalysts and ad-hoc synthesized catalytic systems, respectively.[29,35,37,51] The aim of the present work was not to enter into the debate on the formal oxidation state of the Cr sites active in ethylene polymerization, which is inflaming the literature on the Phillips catalyst in recent times. Rather, we want to shed light on the products of chromates reduction, which remain in the coordination sphere of the reduced Cr sites and participate in the polymerization reaction. We believe that the molecular structure and the ligand sphere of the Cr sites, irrespective of their formal oxidation state, are key players behind the activity towards ethylene and might also explain their tendency toward ethylene polymerization vs oligomerization (i.e. the preference towards propagation vs termination). As a matter of fact, the literature on heterogeneous Cr-based catalysts contains examples of: i) catalysts based on a different Cr oxidation state (Cr^{II} [29,37,75,76] or Cr^{III} [35,36,43,51]) giving a similar polyethylene; and ii) catalysts based on the same Cr oxidation state (either Cr^{II} [90,111,112] or Cr^{III} [51,113,114])[38-40] which either polymerize or oligomerize ethylene. This is true also for homogeneous Cr-based catalysts.[34,115-119] Thus the scientific debate of the Phillips community cannot accommodate a short-sighted discussion centered only on the oxidation state of the active species.

The emerging panorama from this work should set aside the "old" vision of the Phillips catalyst active site constituted by a *naked* (i.e. low coordinated) chromium species, which now appears unrealistic of the reaction taking place in industrial conditions. Rather, external (and flexible) oxygenated ligands seem to be fundamental actors in the polymerization reaction, very much like the ancillary ligands in homogeneous polymerization catalysis. On these basis, external nucleophilic ligands are surely suitable candidates in the *ab-initio* design of Phillips-related olefin polymerization catalysts. The resulting picture coming from this work can be extended also to most of the pre-reducing agents employed on the Cr^{VI}/SiO_2 catalyst, which all act in the same way as pumps of electrons to the chromates, but each one gives a different oxidized product. This might be the reason why each pre-reducing agent gives rise to extremely different catalytic behavior and consequently to different polyethylene products.

4. EXPERIMENTAL SECTION

4.1 Catalyst synthesis and activation. The Cr/SiO_2 catalyst was prepared by wet-impregnation of SiO_2 (aerosil, surface area ca. 360 m^2g^{-1}) with an aqueous solution of CrO_3, having a chromium loading of 1.0 wt%.[9] The chromium loading was kept low enough to avoid segregation of CrO_x during the activation treatments, but sufficiently high to guarantee a good sensitivity with all the techniques. The Cr^{VI}/SiO_2 catalyst was obtained by treating the impregnated sample in the presence of oxygen at 650 °C either in static conditions (two cycles of 30 minutes in pure oxygen, equilibrium pressure 100 mbar) for DR UV-Vis-NIR and FT-IR measurements, or in dynamic conditions (10% O_2 in He, total flow 10 ml/min) for XAS measurements. Reduction of Cr^{VI}/SiO_2 by means of ethylene and subsequent polymerization was achieved by flowing ethylene (pure ethylene 20 ml/min for DR UV-Vis-NIR and FT-IR measurements and pure ethylene in He 10 ml/min for XAS) in the reaction cells at 150 °C. Complementary FT-IR experiments were performed in static conditions ($P_{C_2H_4}$ = 100 mbar). The reference Cr^{II}/SiO_2 catalyst was obtained by reducing the activated Cr^{VI}/SiO_2 sample by means of CO at 350 °C (two cycles of 30 minutes in pure carbon monoxide, equilibrium pressure 100 mbar), and subsequent outgassing at the same temperature.

4.2 Cr K-edge XANES spectroscopy. Cr K-edge XAS spectra were collected at the BM23 beamline at the European Synchrotron Radiation Facility (ESRF, Grenoble, F). The white beam was monochromatized using a Si(111) double crystal and harmonic rejection was performed by using silicon mirrors (4 mrad). The intensity of the incident beam was monitored by an ionization chamber and was vertically focused to a few micron. Due to Cr dilution, EXAFS spectra were collected in fluorescence mode, by means of a 12 element Ge detector. To minimize the elastic scattering a 45° geometry between the incoming X-ray beam and the detector nose was adopted. The samples were measured in the form of powder inside a quartz capillary 1.5 mm in diameter having upstream and downstream two small pieces of quartz wool. The capillary was connected to a gas-dosing system with mass-flow controllers to flow different gas mixtures, and inserted inside a half-circular oven allowing treating the sample up to 650 °C in the presence of different reagents, simultaneously collecting the XAS spectra. XANES spectra were acquired with an energy step of 0.4 eV and an integration time of 2 s/point, up to k = 5 $Å^{-1}$ to allow an easy normalization. Each XANES spectrum required an acquisition time of about 12 minutes as compromise between fast acquisition and quality of the spectra. The XANES spectra were normalized using the Athena program.[116] The evolution of gaseous products of reaction are monitored with online Mass Spectroscopy at the end of the capillary by sampling a fraction of the exit flow.

4.3 DR UV-Vis-NIR spectroscopy. Diffuse reflectance (DR) UV-Vis-NIR spectra were recorded on a Varian Cary5000 instrument on samples in the form of powder placed inside a cell made in suprasil quartz. Sample activation was performed in quartz cylinders in static conditions (two cycles of 30 min in pure O_2, ep = 100 mbar). The activated sample was stocked in a glovebox, and in a second moment transferred inside a DR UV-Vis-NIR cell made in optical quartz (suprasil) and allowing reactions in flow of different gaseous mixtures. The reaction in ethylene was performed by connecting the cell to a gas-dosing system with mass-flow controllers to flow different gas mixtures and inserting the cell inside a circular oven. The spectra were collected in reflectance mode, and successively converted in Kubelka-Munk units. Also in this case we followed the downstream evolution of gaseous products of reaction with online Mass Spectroscopy by sampling a fraction of the exit flow.

4.4 FT-IR spectroscopy. Transmission FT-IR spectra were recorded on a Bruker Vertex70 instrument at 2 cm^{-1} resolution. The catalysts were measured inside a quartz cell equipped with two KBr windows and in the form of thin self-supported pellets. The activation treatments were performed directly in the IR measurement cell in static conditions (two cycles of 30 min in pure O_2, ep = 100 mbar). The measurements during ethylene reduction/polymerization were performed by connecting the cell to a gas-dosing system with mass-flow controllers to flow different gas mixtures. The cell was heated with two glowplugs immersed in silicon carbide powder.

ASSOCIATED CONTENT

Supporting Information. Detailed assignment and discussion of the DR UV-Vis-NIR and FT-IR spectra, along with XANES simulations and DFT-optimized clusters "This material is available free of charge via the Internet at http://pubs.acs.org."

AUTHOR INFORMATION

Corresponding Authors

* Elena Groppo elenagroppo@unito.it
* Caterina Barzan caterinabarzan@unito.it

Funding Sources

Progetto di Ateneo/CSP 2014 (Torino_call2014_L1_73).
Mega-grant of Ministry of Education and Science of the Russian Federation (14.Y26.31.0001)

ACKNOWLEDGMENT

We kindly acknowledge Giovanni Agostini, Sakura Pascarelli and Olivier Mathon for their assistance and expertise during the XAS measurements at BM23 beamline (ESRF in Grenoble). We are grateful to Maria Botavina for the help and discussion on experimental measurements. We thank Alessandro Damin for designing and optimizing the Cr/SiO_2 clusters employed in this work to perform the XANES simulations. A special thanks is devoted to the Emeritus Professor Adriano Zecchina, whose guidance in the field of the Phillips catalyst continuously drives our investigations. Luca Braglia and Carlo Lamberti acknowledge mega-grant of Ministry of Education and Science of the Russian Federation (14.Y26.31.0001). This work has been supported by the Progetto di Ateneo/CSP 2014 (Torino_call2014_L1_73).

REFERENCES

(1) Hogan, J. P.; Banks, R. L. *US. Patent* **1958**, *2.825.721*.
(2) *World Polyethylene, Industry Study with Forecast for 2018 & 2023*; The Freedonia Group: Cleveland, 2014; Study #3210.
(3) McDaniel, M. P. *Adv. Catal.* **2010**, *53*, 123-606.
(4) Nowlin, T. E. *Business and Technology of the Global Polyethylene Industry*; Wiley-Scrivener: New York, 2014.
(5) *Market Report: Global Catalyst Market*; 3d ed. ed.; Acmite Market Intelligence: Ratingen, Germany, 2015.
(6) Weckhuysen, B. M.; Wachs, I. E.; Schoonheydt, R. A. *Chem. Rev.* **1996**, *96*, 3327-3349.
(7) Cheng, R.; Liu, Z.; Zhong, L.; He, X.; Qiu, P.; Terano, M.; Eisen, M. S.; Scott, S. L.; Liu, B. In *Polyolefins: 50 Years after Ziegler and Natta I: Polyethylene and Polypropylene*; Kaminsky, W., Ed.; Spinger-Verlag: Berlin Heidelberg, 2013; Vol. 257, p 135-202.
(8) Liu, Z.; He, X.; Cheng, R.; Eisen, M. S.; Terano, M.; Scott, S. L.; Liu, B. *Adv. Chem. Eng.* **2014**, *44*, 126-191.
(9) Groppo, E.; Lamberti, C.; Bordiga, S.; Spoto, G.; Zecchina, A. *Chem. Rev.* **2005**, *105*, 115-183.

(10) Groppo, E.; Seenivasan, K.; Barzan, C. *Catal. Sci. Technol.* **2013**, *3*, 858-878.
(11) McDaniel, M. P. *J. Catal.* **1981**, *67*, 71-76.
(12) McDaniel, M. P. *J. Catal.* **1982**, *76*, 29-36.
(13) McDaniel, M. P. *J. Catal.* **1982**, *76*, 37-47.
(14) McDaniel, M. P. *J. Catal.* **1982**, *76*, 17-28.
(15) Weckhuysen, B. M.; Deridder, L. M.; Schoonheydt, R. A. *J. Phys. Chem.* **1993**, *97*, 4756-4763.
(16) Weckhuysen, B. M.; Verberckmoes, A. A.; Buttiens, A. L.; Schoonheydt, R. A. *J. Phys. Chem.* **1994**, *98*, 579-584.
(17) Weckhuysen, B. M.; Deridder, L. M.; Grobet, P. J.; Schoonheydt, R. A. *J. Phys. Chem.* **1995**, *99*, 320-326.
(18) Weckhuysen, B. M.; Schoonheydt, R. A.; Jehng, J. M.; Wachs, I. E.; Cho, S. J.; Ryoo, R.; Kijlstra, S.; Poels, E. *J. Chem. Soc. Faraday Trans.* **1995**, *91*, 3245-3253.
(19) Weckhuysen, B. M.; Verberckmoes, A. A.; DeBaets, A. R.; Schoonheydt, R. A. *J. Catal.* **1997**, *166*, 160-171.
(20) Weckhuysen, B. M.; Verberckmoes, A. A.; Debaere, J.; Ooms, K.; Langhans, I.; Schoonheydt, R. A. *J. Mol. Catal. A* **2000**, *151*, 115-131.
(21) Wachs, I. E.; Roberts, C. A. *Chem. Soc. Rev.* **2010**, *39*, 5002-5017.
(22) Chakrabarti, A.; Gierada, M.; Handzlik, J.; Wachs, I. E. *Top. Catal.* **2016**, *59*, 725-739.
(23) Chakrabarti, A.; Wachs, I. E. *Catal. Lett.* **2016**, *145*, 985-994.
(24) Guesmi, H.; Tielens, F. *J. Phys. Chem. C* **2012**, *116*, 994-1001.
(25) Tielens, F.; Islam, M. M.; Skara, G.; De Proft, F.; Shishido, T.; Dzwigaj, S. *Microporous Mesoporous Mat.* **2012**, *159*, 66-73.
(26) Handzlik, J.; Grybos, R.; Tielens, F. *J. Phys. Chem. C* **2013**, *117*, 8138-8149.
(27) Gao, J.; Zheng, Y.; Tang, Y.; Jehng, J.-M.; Grybos, R.; Handzlik, J.; Wachs, I. E.; Podkolzin, S. G. *ACS Catal.* **2015**, *5*, 3078-3092.
(28) Handzlik, J.; Grybos, R.; Tielens, F. *J. Phys. Chem. C* **2016**, *120*, 17594-17603.
(29) Gierada, M.; Michorczyk, P.; Tielens, F.; Handzlik, J. *J. Catal.* **2016**, *340*, 122-135.
(30) Liu, B.; Nakatani, H.; Terano, M. *J. Mol. Catal. A* **2002**, *184*, 387-398.
(31) Liu, B. P.; Nakatani, H.; Terano, M. *J. Mol. Catal. A* **2003**, *201*, 189-197.
(32) Xia, W.; Liu, B. P.; Fang, Y. W.; Hasebe, K.; Terano, M. *J. Mol. Catal. A* **2006**, *256*, 301-308.
(33) Zhong, L.; Liu, Z.; Cheng, R. H.; Tang, S. Y.; Qiu, P. Y.; He, X. L.; Terano, M.; Liu, B. P. *ChemCatChem* **2012**, *4*, 872-881.
(34) McGuinness, D. S. *Chem. Rev.* **2011**, *111*, 2321-2341.
(35) Delley, M. F.; Nunez-Zarur, F.; Conley, M. P.; Comas-Vives, A.; Siddiqi, G.; Norsic, S.; Monteil, V.; Safonova, O. V.; Coperet, C. *Proc. Natl. Acad. Sci.* **2014**, *111*, 11624-11629.
(36) Conley, M. P.; Delley, M. F.; Siddiqi, G.; Lapadula, G.; Norsic, S.; Monteil, V.; Safonova, O. V.; Coperet, C. *Angew. Chem. Int. Ed.* **2014**, *53*, 1872-1876.
(37) Brown, C.; Krzystek, J.; Achey, R.; Lita, A.; Fu, R.; Meulenberg, R. W.; Polinski, M.; Peek, N.; Wang, Y.; de Burgt, L. J.; Profeta, S. J.; Stiegman, A. E.; Scott, S. L. *ACS Catal.* **2015**, *5*, 5574-5583.
(38) Cicmil, D.; Meeuwissen, J.; Vantomme, A.; Wang, J.; van Ravenhorst, I. K.; van der Bij, H. E.; Munoz-Murillo, A.; Weckhuysen, B. M. *Angew. Chem. Int. Ed.* **2015**, *54*, 13073-13079.
(39) Cicmil, D.; Meeuwissen, J.; Vantomme, A.; Weckhuysen, B. M. *ChemCatChem* **2016**, *8*, 1937-1944.
(40) Cicmil, D.; van Ravenhorst, I. K.; Meeuwissen, J.; Vantomme, A.; Weckhuysen, B. M. *Catal. Sci. Technol.* **2016**, *6*, 731-743.
(41) Fong, A.; Peters, B.; Scott, S. L. *ACS Catal.* **2016**, *6*, 6073-6085.
(42) Fong, A.; Yuan, Y.; Ivry, S. L.; Scott, S. L.; Peters, B. *ACS Catal.* **2015**, *5*, 3360-3374.
(43) Conley, M. P.; Delley, M. F.; Nunez-Zarur, F.; Comas-Vives, A.; Coperet, C. *Inorg. Chem* **2015**, *54*, 5065-5078.
(44) Floryan, L.; Borosy, A. P.; Nunez-Zarur, F.; Comas-Vives, A.; Coperet, C. *J. Catal.* **2017**, *346*, 50-56.
(45) Krauss, H. L.; Stach, H. *Inorg. Nucl. Chem.* **1968**, *4*, 393.
(46) Krauss, H. L.; Stach, H. *Z. Anorg. Allg. Chem.* **1969**, *366*, 34-42.
(47) Finch, J. N. *J. Catal.* **1976**, *43*, 111.
(48) Zecchina, A.; Garrone, E.; Ghiotti, G.; Morterra, C.; Borello, E. *J. Phys. Chem.* **1975**, *79*, 966-972.
(49) McDaniel, M. P. *Adv. Catal.* **1985**, *33*, 47-98.
(50) Coperet, C.; Allouche, F.; Chan, K. W.; Conley, M. P.; Delley, M. F.; Fedorov, A.; Moroz, I. B.; Mougel, V.; Pucino, M.; Searles, K.; Yamamoto, K.; Zhizhko, P. A. *Angew. Chem. Int. Ed.* **2017**.
(51) Delley, M. F.; Lapadula, G.; Nunez-Zarur, F.; Comas-Vives, A.; Kalendra, V.; Jeschke, G.; Baabe, D.; Walter, M. D.; Rossini, A. J.; Lesage, A.; Emsey, L.; Maury, O.; Coperet, C. *J. Am. Chem. Soc.* **2017**, *139*, 8855-8867.
(52) Gianolio, D.; Groppo, E.; Vitillo, J. G.; Damin, A.; Bordiga, S.; Zecchina, A.; Lamberti, C. *Chem. Commun.* **2010**, *46*, 976–978.
(53) Corma, A. *Angew. Chem. Int. Ed.* **2016**, 55, 6112-6113.
(54) Schwerdtfeger, E.; Buck, R.; McDaniel, M. *Appl. Catal. A* **2012**, *423*, 91-99.
(55) Barzan, C.; Damin, A. A.; Budnyk, A.; Zecchina, A.; Bordiga, S.; Groppo, E. *J. Catal.* **2016**, *337*, 45-51.
(56) Ajjou, J. A. N.; Scott, S. L. *J. Am. Chem. Soc.* **2000**, *122*, 8968-8976.
(57) Ajjou, J. A. N.; Scott, S. L.; Paquet, V. *J. Am. Chem. Soc.* **1998**, *120*, 415-416.
(58) Bordiga, S.; Groppo, E.; Agostini, G.; van Bokhoven, J. A.; Lamberti, C. *Chem. Rev.* **2013**, *113*, 1736-1850.
(59) Lamberti, C.; Zecchina, A.; Groppo, E.; Bordiga, S. *Chem. Soc. Rev.* **2010**, *39*, 4951–5001.
(60) Singh, J.; Lamberti, C.; van Bokhoven, J. A. *Chem. Soc. Rev.* **2010**, *39*, 4754-4766.
(61) Chakrabarti, A.; Ford, M. E.; Gregory, D.; Hu, R.; Keturakis, C. J.; Lwin, S.; Tang, Y.; Yang, Z.; Zhu, M.; Banares, M. A.; Wachs, I. E. *Catal. Today* **2017**, *283*, 27-53.
(62) Vimont, A.; Thibault-Starzyk, F.; Daturi, M. *Chem. Soc. Rev.* **2010**, *39*, 4928-4950.
(63) Dou, J.; Sun, Z.; Opalade, A. A.; Wang, N.; Fu, W.; Tao, F. *Chem. Soc. Rev.* **2017**, *46*, 2001-2027.
(64) The temperature of 150 °C adopted in this work is slightly higher with respect to the one used in industrial conditions. This correction was necessary to compensate for the low ethylene pressure employed in our experimental conditions.
(65) Fubini, B.; Ghiotti, G.; Stradella, L.; Garrone, E.; Morterra, C. *J. Catal.* **1980**, *66*, 200-213.
(66) Weckhuysen, B. M.; Schoonheydt, R. A. *Catal. Today* **1999**, *49*, 441-451.
(67) Engemann, C.; Hormes, J.; Longen, A.; Dotz, K. H. *Chem. Phys.* **1998**, *237*, 471-481.
(68) Pantelouris, A.; Modrovw, H.; Pantelouris, M.; Hormes, J.; Reinen, D. *Chem. Phys.* **2004**, *300*, 13-22.
(69) Demmelmaier, C. A.; White, R. E.; van Bokhoven, J. A.; Scott, S. L. *J. Phys. Chem. C* **2008**, *112*, 6439-6449.

(70) Demmelmaier, C. A.; White, R. E.; van Bokhoven, J. A.; Scott, S. L. *J. Catal.* **2009**, *262*, 44-56.

(71) Groppo, E.; Prestipino, C.; Cesano, F.; Bonino, F.; Bordiga, S.; Lamberti, C.; Thüne, P. C.; Niemantsverdriet, J. W.; Zecchina, A. *J. Catal.* **2005**, *230*, 98-108.

(72) Tromp, M.; Moulin, J. O.; Reid, G.; Evans, J. *AIP Conf. Proc.* **2007**, *882*, 699-701.

(73) Heating the catalyst/polymer composite in O_2 gave CO and CO_2 as the main oxidation by-products, as revealed by online MS.

(74) Groppo, E.; Lamberti, C.; Bordiga, S.; Spoto, G.; Zecchina, A. *J. Phys. Chem. B* **2005**, *109*, 15024-15031.

(75) Groppo, E.; Lamberti, C.; Cesano, F.; Zecchina, A. *Phys. Chem. Chem. Phys.* **2006**, *8*, 2453-2456.

(76) Groppo, E.; Lamberti, C.; Bordiga, S.; Spoto, G.; Zecchina, A. *J. Catal.* **2006**, *240*, 172-181.

(77) Groppo, E.; Estephane, J.; Lamberti, C.; Spoto, G.; Zecchina, A. *Catal. Today* **2007**, *126*, 228-234.

(78) Groppo, E.; Damin, A.; Otero Arean, C.; Zecchina, A. *Chem. Eur. J.* **2011**, *17*, 11110 – 11114.

(79) Chelazzi, D.; Ceppatelli, M.; Santoro, M.; Bini, R.; Schettino, V. *Nat. Mater.* **2004**, *3*, 470-475.

(80) Delley, M. F.; Conley, M. P.; Coperet, C. *Catal. Lett.* **2014**, *144*, 805-808.

(81) Fackler, J.; Holan, D. *Inorg. Chem* **1964**, *4*, 954-958.

(82) Figgis, B. N. *Introduction to ligand fields*; John Wiley & Sons: New York, 1966.

(83) Clark, R. J. H. *J. Chem. Soc.* **1964**, *0*, 417-425.

(84) Note that the band centered at ca. 9500 cm^{-1} corresponds to a very broad band centered at 1050 nm. Since most of literature spectra are shown in the 200-800 nm range, this band and similar ones cannot be measured. In addition, reporting the spectra in wavenumbers (which is the most correct way, being wavenumbers directly proportional to the energy of the transition) allows to define the maximum of d-d bands which would be too broad in wavelength.

(85) Crocella, V.; Cerrato, G.; Magnacca, G.; Morterra, C.; Cavani, F.; Maselli, L.; Passeri, S. *Dalt. Trans.* **2010**, *39*, 8527-8537.

(86) Busca, G.; Lorenzelli, V. *J. Catal.* **1980**, *66*, 155-166.

(87) Busca, G.; Lamotte, J.; Lavalley, J. C.; Lorenzelli, V. *J. Am. Chem. Soc.* **1987**, *109*, 5197-5202.

(88) Vijayaraj, M.; Gopinath, C. S. *J. Catal.* **2004**, *226*, 230-234.

(89) Busca, G. *Catal. Today* **1996**, *27*, 457-496.

(90) Barzan, C.; Groppo, E.; Quadrelli, E. A.; Monteil, V.; Bordiga, S. *Phys. Chem. Chem. Phys.* **2012**, *14*, 2239-2245.

(91) Spoto, G.; Bordiga, S.; Ricchiardi, G.; Scarano, D.; Zecchina, A.; Borello, E. *J. Chem. Soc. Faraday Trans.* **1994**, *90*, 2827-2835.

(92) Cieslak-Golonka, M. *Coordin. Chem. Rev.* **1991**, *109*, 223-249.

(93) Ooi, T.; Miura, T.; Itagaki, Y.; Ichikawa, I.; Maruoka, K. *Synthesis-Stuttgart* **2002**, 279-291.

(94) Mojtahedi, M. M.; Akbarzadeh, E.; Sharifi, R.; Abaee, M. S. *Org. Lett.* **2007**, *9*, 2791-2793.

(95) Gnanadesikan, V.; Horiuchi, Y.; Ohshima, T.; Shibasaki, M. *J. Am. Chem. Soc.* **2004**, *126*, 7782-7783.

(96) Hoshimoto, Y.; Ohashi, M.; Ogoshi, S. *J. Am. Chem. Soc.* **2011**, *133*, 4668-4671.

(97) Curran, S. P.; Connon, S. J. *Angew. Chem. Int. Ed.* **2012**, *51*, 10866-10870.

(98) Lochar, V. *Appl. Catal., A* **2006**, *309*, 33-36.

(99) Joly, Y. *Phys. Rev. B* **2001**, *63*, art. no. 125120.

(100) Guda, S. A.; Guda, A. A.; Soldatov, M. A.; Lomachenko, K. A.; Bugaev, A. L.; Lamberti, C.; Gawelda, W.; Bressler, C.; Smolentsev, G.; Soldatov, A. V.; Joly, Y. *J. Chem. Theory Comput.* **2015**, *11*, 4512-4521.

(101) Guda, A. A.; Guda, S. A.; Soldatov, M. A.; Lomachenko, K. A.; Bugaev, A. L.; Lamberti, C.; Gawelda, W.; Bressler, C.; Smolentsev, G.; Soldatov, A. V.; Joly, Y. *J. Phys.: Conf. Ser.* **2016**, *712*, Article N. 012004.

(102) Bunau, O.; Joly, Y. *J. Phys.-Condes. Matter* **2009**, *21*.

(103) Smolentsev, G.; Soldatov, A. V.; Joly, Y.; Pascarelli, S.; Aquilanti, G. *Radiat. Phys. Chem.* **2006**, *75*, 1571-1573.

(104) Joly, Y.; Greiner, S. In *Theory of X-Ray Absorption Near Edge Structure.*; Sons, E. J. W., Ed. Chichester (UK), 2016; Vol. I, p 73-97.

(105) Note that the employed models contain more than 80 atoms in oder to simulate a substantial portion of the silica support, which is known to affect the strain at the Cr sites.

(106) Notably, the main message coming from XANES spectral comparison and simulation is that the assignment of the Cr oxidation state by XANES spectroscopy is not unambiguous, as pointed in the past (72) but often neglected, and it should be assisted by theoretical calculation and taking into account any additional information obtained by complementary characterization techniques.

(107) Potter, K. C.; Beckerle, C. W.; Jentoft, F. C.; Schwerdtfeger, E.; McDaniel, M. P. *J. Catal.* **2016**, *344*, 657-668.

(108) Liu, B. P.; Sindelar, P.; Fang, Y. W.; Hasebe, K.; Terano, M. *J. Mol. Catal. A* **2005**, *238*, 142-150.

(109) Cheng, R. H.; Xu, C.; Liu, Z.; Dong, Q.; He, X. L.; Fang, Y. W.; Terano, M.; Hu, Y. T.; Pullukat, T. J.; Liu, B. P. *J. Catal.* **2010**, *273*, 103-115.

(110) Amakawa, K.; Sun, L.; Guo, C.; Hävecker, M.; Kube, P.; Wachs, I.E.; Lwin, S.; Frenkel, A.I.; Patlolla, A.; Hermann, K.; Schlögl, R.; Trunschke, A. *Angew. Chem. Int. Ed.* **2013**, *52*, 13553-13557.

(111) Barzan, C.; Gianolio, D.; Groppo, E.; Lamberti, C.; Monteil, V.; Quadrelli, E. A.; Bordiga, S. *Chem. Eur. J.* **2013**, *19*, 17277-17282.

(112) Monoi, T.; Sasaki, Y. *J. Mol. Catal. A* **2002**, *187*, 135-141.

(113) Monoi, T.; Ikeda, H.; Ohira, H.; Sasaki, Y. *Polym. J.* **2002**, *34*, 461-465.

(114) Nenu, C. N.; Bodart, P.; Weckhuysen, B. M. 2005.

(115) Vidyaratne, I.; Nikiforov, G. B.; Gorelsky, S. I.; Gambarotta, S.; Duchateau, R.; Korobkov, I. *Angew. Chem., Int. Ed.* **2009**, *48*, 6552.

(116) Jabri, A.; Mason, C. B.; Sim, Y.; Gambarotta, S.; Burchell, T. J.; Duchateau, R. *Angew. Chem.-Int. Edit.* **2008**, *47*, 9717-9721.

(117) Albahily, K.; Koc, E.; Al-Baldawi, D.; Savard, D.; Gambarotta, S.; Burchell, T. J.; Duchateau, R. *Angew. Chem.-Int. Edit.* **2008**, *47*, 5816-5819.

(118) Yang, Y.; Gurnham, J.; Liu, B. P.; Duchateau, R.; Ganabarotta, S.; Korobkov, I. *Organometallics* **2014**, *33*, 5749-5757.

(119) Ravel, B.; Newville, M. *J. Synchrot. Radiat.* **2005**, *12*, 537-541.